EEET ECOLOGICAL ENGINEERING & ENVIRONMENTAL TECHNOLOGY

Ecological Engineering & Environmental Technology, 2026, 27(7), 175–185
https://doi.org/10.12912/27197050/222624
ISSN 2719–7050, License CC-BY 4.0

Received: 2026.05.14
Accepted: 2026.06.15
Published: 2026.07.01

Monodisperse silver nanoparticles synthesized via citrate-glycerol route: An efficient catalytic system for 4-nitrophenol reduction

Thuy-An Nguyen[1,2], Ngoc-Tram-Anh Tran[1,2], Thi-Kim-Hoang Le[1,2], Hoa-Hung Lam[1,2], Trung Dang-Bao[1,2*]

[1] Faculty of Chemical Engineering, Ho Chi Minh City University of Technology (HCMUT), 268 Ly Thuong Kiet Street, Dien Hong Ward, Ho Chi Minh City, Vietnam
[2] Vietnam National University Ho Chi Minh City, Linh Xuan Ward, Ho Chi Minh City, Vietnam
* Corresponding author's e-mail: dbtrung@hcmut.edu.vn

ABSTRACT

This study presents a "modified polyol" approach for the synthesis of silver nanoparticles (AgNPs) utilizing a synergistic citrate-glycerol system. Glycerol functions as a non-toxic solvent, mild co-reductant, and stabilizing medium, while citrate serves as a secondary stabilizer to ensure colloidal stability through electrostatic repulsion. The formation of AgNPs were systematically monitored via UV-Vis spectroscopy to determine optimal synthetic parameters. The crystalline structure, surface chemistry, and morphological attributes of the synthesized nanoparticles were systematically characterized using X-ray diffraction (XRD), selected area electron diffraction (SAED), Fourier transform infrared spectroscopy (FTIR), and transmission electron microscopy (TEM), confirming the production of phase-pure silver crystals with a spherical morphology and a well-defined average diameter of 9.5 nm. The catalytic evaluation of AgNPs was evaluated through the aqueous reduction of 4-nitrophenol (4-NP) to 4-aminophenol (4-AP) utilizing $NaBH_4$. Using a low catalyst loading of 0.10 ppm, a 92% degradation efficiency was achieved within 6 minutes. Kinetic analysis followed a pseudo-first-order model, yielding an apparent rate constant of 0.4673 ± 0.0095 min^{-1} (n = 3). These results underscore their high catalytic activity, positioning this sustainable synthesis for pollutant removal and the transformation of toxic industrial waste into valuable chemical precursors.

Keywords: silver nanoparticles, glycerol, sustainable synthesis, nanocatalysis, 4-nitrophenol.

INTRODUCTION

The rapid evolution of metal nanoparticle fabrication has recently changed how we approach organic pollutant treatment (Boulkhessaim et al., 2022; Tran et al., 2025), antimicrobial medicine (Tripathi et al., 2022; Nguyen et al., 2025), and environmental sensing (Dang-Bao et al., 2023; Nguyen-Huynh et al., 2025). This technological shift is rooted in the unique physical phenomena, such as size and surface effects, that emerge as materials are scaled down to the nanometer level (Jamkhande et al., 2019). In catalysis, nanoparticles effectively bridge the traditional gap between homogeneous and heterogeneous systems. However, the practical utility of these nanocatalysts depends on governing their size, morphology, and dispersion (Dang-Bao et al., 2021). A challenge remains the thermodynamic tendency of nanoparticles to aggregate into bulk clusters, which drastically reduces active surface area and catalytic performance. Consequently, designing efficient systems requires a balance of stabilizers or solid supports to maintain the integrity of the metallic phase.

In this context, silver nanoparticles (AgNPs) command significant attention owing to their remarkable catalytic power (Ly et al., 2024; Kumar et al., 2025) and antibacterial properties (Bruna et al., 2021; Selvam et al., 2026). Many researchers have turned to biosynthesis using plant extracts as an eco-friendly alternative; however, these methods frequently lack reproducibility (Moradi et al., 2021; Phan et al., 2024). The inherent complexity of plant chemistry makes it difficult to regulate

nucleation and growth, often leading to polydisperse products. On the other hand, conventional chemical reduction offers tighter control but relies on aggressive reductants like sodium borohydride or hydrazine. These chemicals present not only a high toxicity risk to researchers but also significant environmental disposal challenges.

Polyol protocols have long served as a key strategy, mainly relying on ethylene glycol that act as weak reductants under severe thermal conditions. For example, Kästner and Thünemann (2016) and Wolf et al. (2022) fabricated spherical AgNPs (~5-6 nm) in ethylene glycol utilizing poly(acrylic acid) stabilizers at high temperatures (up to 210 °C). Similarly, when non-ionic polymers like polyvinylpyrrolidone (PVP) are introduced for steric shielding, high thermal thresholds and prolonged holding times remain mandatory; this is evident in microwave-assisted systems at 160 °C yielding 80-120 nm structures (Helmlinger et al., 2015), and conventional heating treatments at 120-160 °C generating widely dispersed particles up to 200 nm (Ahmad et al., 2024; Zhao et al., 2010). Collectively, these conventional polyol routes have been carried out at high temperatures, while AgNPs fabrication remains on ethylene glycol, with glycerol-mediated routes rarely explored.

In contrast, standard aqueous reductions utilizing trisodium citrate typically operate under milder conditions where citrate functions concurrently as a weak reductant and an electrostatic capper. While capable of generating AgNPs, with reported average dimensions from 6 nm (Oprica et al., 2020) up to 38.47 nm (Tessema et al., 2023) and 50 nm (Mohaghegh et al., 2020), these aqueous configurations lack structural matrix entrapment. Consequently, the emerging metallic colloids remain highly susceptible to long-term Ostwald ripening, unconstrained secondary growth, and irreversible aggregation.

In this study, we presents a "modified polyol" approach using a dual citrate-glycerol system. Within this dual framework, glycerol operates as a non-toxic solvent, mild co-reductant, and viscous stabilizing medium (Dang-Bao et al., 2022; Tran et al., 2025); its high viscosity is uniquely advantageous for kinetic regulation, limiting precursor diffusion throughout the polyol matrix to yield highly monodispersed particles with narrow size distributions (Dong et al., 2015; Fiévet et al., 2018). Concurrently, trisodium citrate acts as a secondary capper, imparting immediate electrosteric repulsion that keeps the un-agglomerated nanoparticle surfaces isolated and highly catalytically active.

The synthesized AgNPs was tested through the selective reduction of 4-nitrophenol (4-NP) into 4-aminophenol (4-AP) in water. 4-NP is a stubborn organic pollutant common in pharmaceutical and pesticide manufacturing. Its stability in water and high toxicity make it a severe threat to aquatic life and human health (Zhang et al., 2022; Wang et al., 2025). Interestingly, its reduction product (4-AP) is a valuable chemical intermediate used in the synthesis of analgesics like paracetamol (Mejía and Bogireddy, 2022). Therefore, this research presents a sustainable synthesis method, offering an pollutant removal tool that simultaneously transforms a toxic pollutant into a high-value industrial precursor.

EXPERIMENTAL

Fabrication of monodisperse AgNPs via citrate-glycerol route

The fabrication of AgNPs was achieved through a modified polyol route. In a representative synthesis, a 10 mL glycerol (99.0%, Fisher) solution was prepared, containing 1 mM silver nitrate ($AgNO_3$, 99.8%, Fisher) and 5 mM trisodium citrate (TSC, 99.0%, Xilong) as the dual-functional reducing and stabilizing agents. The mixture was subjected to continuous magnetic stirring at a constant temperature of 100 °C for a duration of 30 min. The reduction of Ag^+ species to Ag^0 and the subsequent nucleation of AgNPs were visually monitored by the distinct color transition of the medium from a transparent state to a characteristic yellow hue, signifying the excitation of surface plasmon resonance.

To identify the ideal conditions for particle formation, several key parameters were systematically varied. These included the reaction duration (ranging up to 60 min), thermal conditions (varying between 60 and 140 °C), and the stoichiometric molar ratio of silver to citrate ([Ag]/[TSC]), which was adjusted across a range from 1/0 to 1/9. Furthermore, to evaluate the specific influence of the polyol matrix on the growth and stabilization of the particles, the optimized protocol was replicated by substituting glycerol with alternative media, specifically deionized water, ethylene glycol, and propylene glycol.

Following the thermal treatment, the colloidal suspensions were allowed to cool naturally to room temperature and were stored under ambient conditions for subsequent characterization. For the acquisition of solid-phase AgNPs, the particles were isolated from the viscous glycerol matrix via high-speed centrifugation. The resulting precipitates were subjected to multiple washing cycles using distilled water and ethanol to ensure the removal of residual precursors and glycerol. Finally, the purified AgNPs were air-dried at room temperature overnight before further analysis.

Reduction kinetics of 4-NP to 4-AP in water using AgNPs nanocatalysts

The catalytic performance was assessed through a benchmark reduction assay conducted in a 1.0 cm path-length quartz cuvette at ambient temperature. The reaction mixture, with a total volume of 3.0 mL, was prepared by combining a 20 ppm aqueous solution of 4-NP (99.0%, HiMedia) with a freshly prepared $NaBH_4$ (99.0%, Xilong) solution, maintained at a high molar excess ([$NaBH_4$]/[4-NP] = 175/1). To initiate the catalytic process, AgNPs were introduced into the system at a final concentration of 0.10 ppm. The chemical transformation was monitored in-situ using an Optizen POP UV–Vis spectrophotometer, recording the absorbance spectra within the 200-600 nm range. Data points were collected at 2-minute intervals, continuing until the complete decolorization of the yellow solution, which indicated the total conversion of the 4-nitrophenolate species.

To evaluate the specific parameters influencing catalytic efficiency, a systematic variation of experimental factors was conducted. In these controlled trials, a single independent variable (such as reaction time, reactant concentration, and catalyst dosage) was modified while all other parameters remained fixed according to the aforementioned baseline protocol.

The reaction kinetics for the catalytic reduction of 4-NP were evaluated by analyzing the linear relationship between $\ln(C_t/C_0)$ and the reaction time (t). Given that the concentration of $NaBH_4$ was maintained at a substantial stoichiometric excess relative to the 4-NP substrate, the reaction was assumed to follow pseudo-first-order kinetics: $\ln(C_t/C_0) = -kt$. In this model, C_0 and C_t represent the concentration of 4-NP at the initial state and at a specific time interval (t), respectively. The efficiency of the process is quantified by the apparent rate constant (k), derived from the slope of the linear regression.

RESULTS AND DISCUSSION

Investigation of synthetic parameters governing the formation of AgNPs in glycerol

The evolution of AgNPs within the citrate-glycerol matrix was systematically monitored via UV-Vis spectroscopy (Figure 1). The initial precursor solution, containing $AgNO_3$ and glycerol, was colorless. Upon heating to 100 °C (at a fixed [Ag]/[TSC] molar ratio of 1/5), a distinct chromatic transition to a pale yellow was observed, intensifying as the reaction progressed. This optical change serves as a qualitative indicator of the chemical reduction of Ag^+ to Ag^0 and the subsequent nucleation of silver clusters (Phan et al., 2024; Nguyen et al., 2025).

Spectroscopically, this process was characterized by the emergence of a prominent absorption maximum (λ_{max}) at 408 nm, contributed by the surface plasmon resonance (SPR) of silver nanospheres (Phan et al., 2024; Nguyen et al., 2025). The absorbance intensity exhibited a temporal increase, reaching a maximum peak at the 30-minute mark (Figure 1a). This peak profile suggests that the nucleation and growth kinetics reached an equilibrium, yielding a highly stable colloidal suspension. Beyond this optimal duration, a decline in absorbance intensity was noted, likely associated with Ostwald ripening or particle coalescence, which reduces the concentration of monodisperse AgNPs (Thanh et al., 2014; Polte, 2015). Consequently, 30 minutes was established for optimal particle density.

The impact of temperature (60-140 °C) on the synthesis was similarly evaluated (Figure 1b). While the λ_{max} remained consistent at 408 nm, confirming the persistence of spherical morphologies; the reaction efficiency was highly temperature-dependent. At a lower temperature (60 °C), the SPR signal remained negligible, indicating insufficient Ag^+ reduction. The highest optical density and narrowest full-width at half-maximum (FWHM) were achieved at 100 °C, signifying the formation of high-density, well-dispersed nanoparticles. Conversely, temperatures exceeding 120 °C resulted in peak broadening and a reduction in absorbance. This phenomenon is attributed to the excessive kinetic energy within the

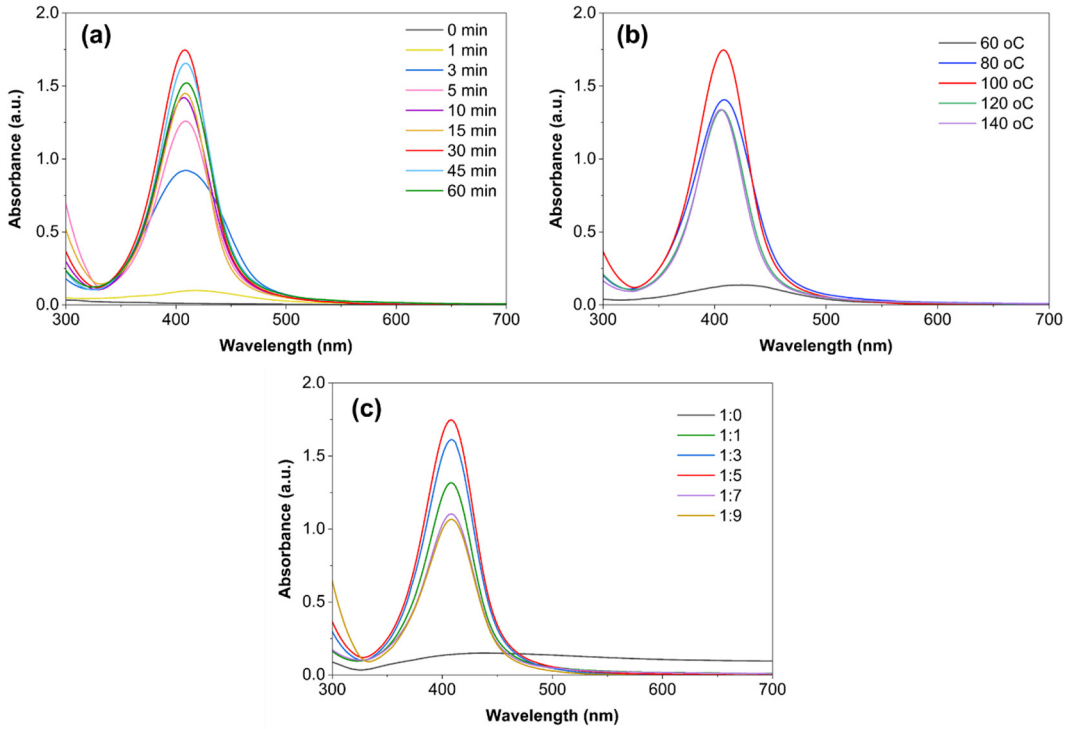

Figure 1. UV-Vis absorption spectra of AgNPs synthesized in citrate-glycerol, showing the influence of (a) reaction time, (b) reaction temperature, and (c) [Ag]/[TSC] molar ratio (recorded following a 15-fold dilution)

system, which accelerates inter-particle collisions and promotes uncontrollable agglomeration (Le et al., 2025; Nguyen et al., 2025).

The TSC role was investigated by varying the [Ag]/[TSC] molar ratio from 1/1 to 1/9 (Figure 1c). While all configurations exhibited the characteristic 408 nm SPR peak, the maximum absorbance was recorded at a 1/5 ratio. This stoichiometry appears to provide a sufficient concentration of citrate ions to facilitate complete Ag^+ reduction (Oprica et al., 2020). Furthermore, TSC serves as a secondary stabilizing agent, imparting the requisite electrostatic repulsion to prevent particle coalescence. At sub-optimal TSC levels, the insufficient capping density led to poor colloidal stability. Interestingly, a surplus of TSC (above the 1/5 ratio) resulted in a decreased absorbance signal, due to an increase in the ionic strength of the medium or background scattering effects from excess species. Crucially, the control experiment conducted in the absence of citrate (a ratio of 1/0) confirm that glycerol alone possesses insufficient reducing capacity to transform Ag^+ into Ag^0 under identical conditions.

Based on these spectroscopic findings, the optimized parameters were determined to be a reaction time of 30 minutes, a temperature of 100 °C, and an [Ag]/[TSC] molar ratio of 1/5.

Impact of glycerol on the colloidal stability and crystalline structure of AgNPs

Glycerol functions as a dual-purpose medium in the AgNPs fabrication, acting as both solvent and stabilizers. Its effectiveness is attributed to high polarity, a trivalent hydroxyl structure, and a substantial dynamic viscosity (~1410 mPa·s at 25 °C). These attributes facilitate stabilization through electrostatic forces and hydrogen bonding, while the high viscosity physically hinders the agglomeration rate, ensuring consistent particle growth and good dispersity (Dang-Bao et al., 2022; Le et al., 2025).

Comparative studies involving water, ethylene glycol (EG), and propylene glycol (PG) highlight the good performance of glycerol (GL). In Figure 2a, only the citrate-glycerol system produces an intense, sharp SPR peak blueshifted to 408 nm. In contrast, the alternative solvents yield negligible absorption, signifying poor formation efficiency and colloidal instability. When compared to a conventional aqueous reduction control consisting of a citrate-water mixture, the dual

matrix demonstrates clear operational superiority. Although the aqueous citrate is capable of reducing Ag^+ ions, it produces a weak, broad SPR band redshifted toward approximately 430 nm. Transitioning to the dual citrate-glycerol framework enhances the reduction efficiency, yielding a much higher particle density and a smaller particle size.

According to Figures 1c and 2a, the control data show that glycerol is independently incapable of reducing Ag^+ ions due to thermodynamic limitations; however, its integration alongside citrate alters the nucleation and growth kinetics. Within the citrate-glycerol framework, citrate initiates rapid chemical reduction while providing electrosteric shielding to the nuclei. Concurrently, the extended carbon chain, high viscosity, and triple hydroxyl groups of glycerol establish a hydrogen-bonded network (Dang-Bao et al., 2022; Nguyen et al., 2025). This structure acts as a physical kinetic barrier that traps and stabilizes the growing silver clusters.

The stability of AgNPs in the citrate-glycerol matrix was demonstrated by the time-resolved UV-Vis profiles (Figure 2b). The SPR intensity of the nano-colloid remained after 30 days of ambient storage. This negligible spectral difference underscores the good stability and resistance to degradation achieved by the dual-stabilizer framework. It is likely that citrate molecules provide immediate electrosteric repulsion at the core boundaries, a glycerol shell effectively envelopes AgNPs. This surrounding polyol matrix establishes a physical barrier that systematically suppresses particle agglomeration and limits inter-particle diffusion.

The crystalline structure, surface chemistry, and morphological attributes of AgNPs were characterized using X-ray diffraction (XRD), selected area electron diffraction (SAED), Fourier transform infrared spectroscopy (FT-IR), and transmission electron microscopy (TEM).

XRD pattern (Figure 3a) confirmed the presence of phase-pure silver (Ag^0), with distinct diffraction peaks corresponding to the (111), (200), (220), and (311) planes. These reflections align with the face-centered cubic (FCC) lattice structure of silver (JCPDS 87-0719 standard). FT-IR analysis of the solid-state AgNPs confirmed the coordination of citrate molecules on the metallic surface (Figure 3b). Specifically, the spectrum displays a broad band at 3434 cm^{-1} corresponding to the -OH stretching vibration, alongside distinct peaks at 1592 cm^{-1} and 1397 cm^{-1} assigned to the asymmetric and symmetric stretching modes of the carboxylate (COO^-) groups, respectively (Shahbazi and Zare-Dorabei, 2019). Crucially, the absorption bands observed at 1276 cm^{-1} and 1080 cm^{-1} are attributed to the C-O stretching vibrations of the polyol backbone and aliphatic ether linkages, confirming the structural integration of glycerol within the capping layer (Le et al., 2025). Furthermore, the band at 620 cm^{-1} is associated with the bending vibrations of the carboxylate groups and the skeletal coordination of Ag-O complexes, verifying the chemisorption of the stabilizers onto the particle surface.

TEM imaging (Figure 3c) and the corresponding particle size distribution histogram (Figure 3d) revealed a highly uniform population of spherical, monodispersed nanoparticles. The fabricated clusters exhibit a well-defined size distribution centered at an average diameter of 9.5 nm. This narrow polydispersity index demonstrates that the synthesis parameters effectively regulated the crystal growth and stabilization kinetics. Furthermore, SAED analysis (Figure 3e) elucidates the crystallographic nature of AgNPs,

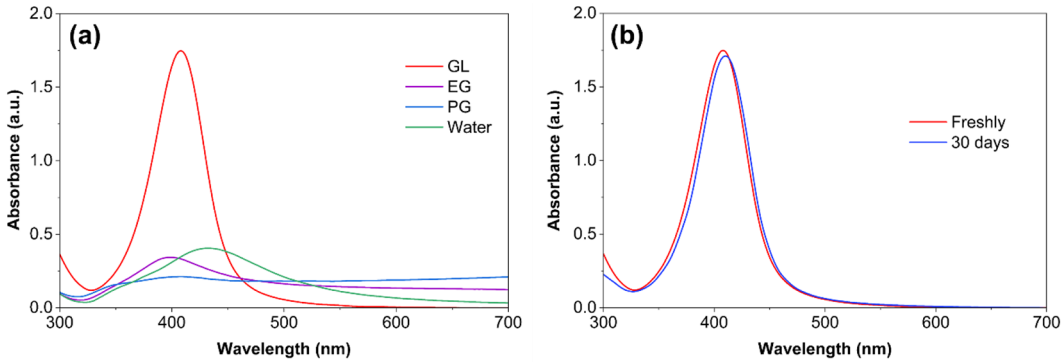

Figure 2. UV-Vis absorption spectra of (a) AgNPs synthesized in various citrate-solvents and (b) stability of AgNPs in citrate-glycerol over 30 days

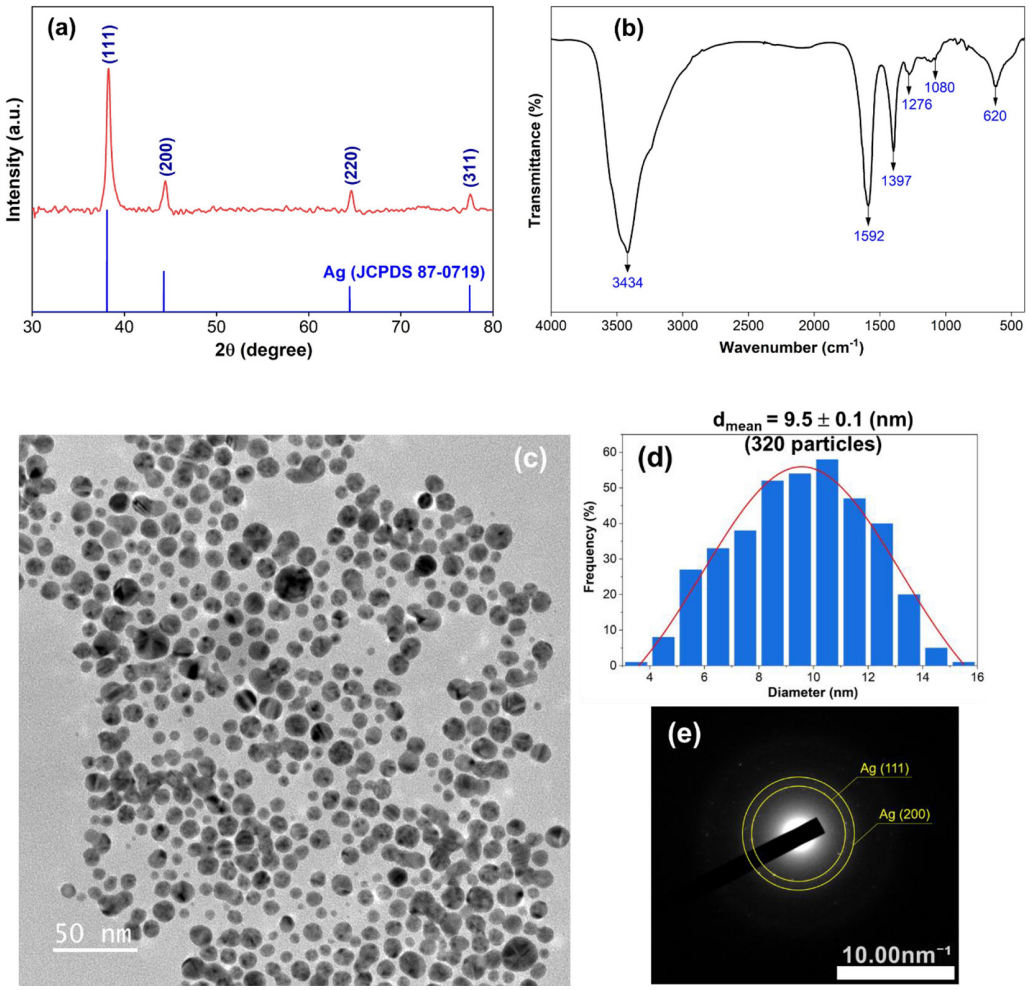

Figure 3. (a) XRD pattern, (b) FTIR spectrum, (c) TEM image, (d) particle size distribution, and (e) SAED pattern of AgNPs synthesized in citrate-glycerol

displaying distinct diffraction rings indexed to the (111) and (200) reflection planes. These orientations confirm the FCC lattice structure, which is in good agreement with the bulk crystallinity determined by XRD (Figure 3a). Such precisely tailored, small-scale spherical configurations maximize the density of surface-active facets, rendering them highly advantageous for catalytic applications.

Catalytic efficiency and kinetic studies of AgNPs in the reduction of 4-NP to 4-AP

The catalytic efficiency of AgNPs was assessed via the aqueous reduction of 4-NP to 4-AP at room temperature, utilizing $NaBH_4$ as the reducing agent. 4-NP is a persistent organic contaminant common in pharmaceutical and pesticide runoff, posing severe ecological risks due to its toxicity and stability (Zhang et al., 2022; Wang et al., 2025). However, its reduction yields 4-AP, a high-value industrial precursor for analgesics like paracetamol (Mejía and Bogireddy, 2022). Consequently, this approach serves as both a remediation tool and a sustainable chemical transformation.

The catalytic process follows the Langmuir–Hinshelwood model, where 4-NP first undergoes deprotonation in the alkaline medium to form 4-nitrophenolate ions. These ions, along with borohydride-derived species, adsorb onto the Ag-NPs active sites, facilitating the electron transfer to the nitro group. This specific pathway ensures the exclusive formation of 4-AP without intermediate byproducts (Das and Das, 2022; Sharma et al., 2024). Using a stoichiometric excess of $NaBH_4$, the reaction kinetics can be described using a pseudo-first-order model (Mejía and Bogireddy, 2022; Thach-Nguyen et al., 2022).

In this work, the catalytic reduction of 4-NP to 4-AP was monitored via UV-Vis spectroscopy in an aqueous medium at room temperature using

$NaBH_4$. Upon the addition of 0.10 ppm of AgNPs catalyst, a progressive decline in the characteristic absorption peak of 4-nitrophenolate at 400 nm (associated with the yellow alkaline solution) was accompanied by a concomitant rise in a new peak at 300 nm, corresponding to the formation of the colorless 4-aminophenolate (Figure 4a). The appearance of two distinct isosbestic points at 280 nm and 320 nm confirms the stoichiometric conversion of 4-NP to 4-AP, indicating a clean transformation without the formation of secondary by-products (Ayad et al., 2020; Thach-Nguyen et al., 2022). Within 6 minutes, a degradation efficiency of 92% was achieved, as evidenced by the complete decolorization of the reaction mixture.

$NaBH_4$ was found as the hydrogen source for such a reduction. In the absence of $NaBH_4$, no conversion was observed; however, increasing the $NaBH_4$ dosage enhanced the reaction rate, as shown by the accelerated depletion of the 400 nm peak within the 6-minute timeframe (Figure 4b). It is worth noting that while higher reductant concentrations drive the reaction, the excessive generation of hydrogen bubbles on the AgNPs surfaces can partially passivate active sites, slightly moderating the rate of electron transfer (Neal et al., 2019). Based on these observations, a $[NaBH_4]/[4\text{-NP}]$ molar ratio of 175/1 was identified as optimal for the 6-minute interval.

The catalyst role of AgNPs is further illustrated in Figure 4c. Without the addition of AgNPs, the 400 nm absorption peak remained static, confirming that no reduction was observed despite the presence of $NaBH_4$. Increasing the catalyst loading led to a significant decrease in the absorption intensity, reflecting an accelerated reaction rate.

To quantify the catalytic performance, the reaction kinetics were analyzed using a pseudo-first-order model, justified by the high stoichiometric excess of $NaBH_4$ (175/1) relative to 4-NP. The apparent rate constants (k) were derived from the slope of the linear plots of $\ln(C_t/C_0)$ versus time (Figure 4d). The calculated k values increased proportionally with catalyst concentration: 0.1097 min^{-1} (0.05 ppm), 0.4584 min^{-1} (0.10 ppm), 0.6680 min^{-1} (0.15 ppm), and 1.3205 min^{-1} (0.20 ppm), demonstrating the high efficiency and concentration-dependent activity of AgNPs in this reduction.

Table 1 provides a comparison of the catalytic performance of the dual-stabilized citrate-glycerol AgNPs against previously reported silver-based catalysts evaluated for the ambient reduction of 4-NP to 4-AP in the presence of $NaBH_4$. Notably, the AgNPs synthesized via this modified polyol

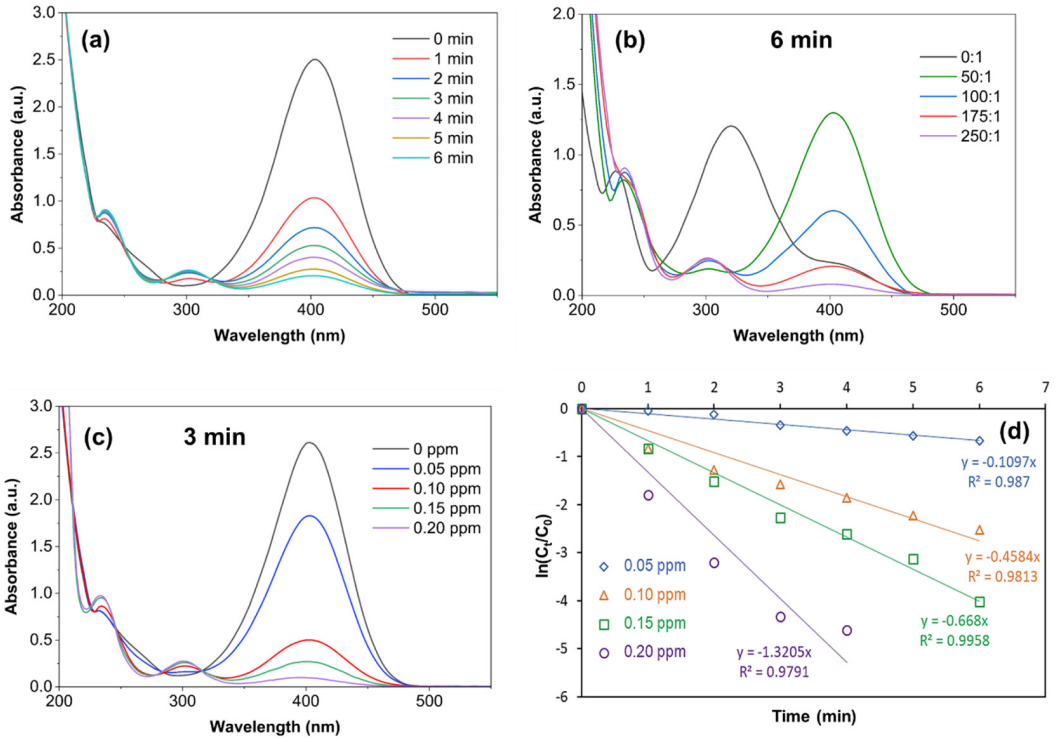

Figure 4. Reductive transformation of 4-NP to 4-AP catalyzed by AgNPs at ambient temperature influenced by (a) reaction time, (b) $[NaBH_4]/[4\text{-NP}]$, (c) silver concentration, and (d) pseudo-first-order kinetic analysis

Table 1. Catalytic efficiency of citrate-glycerol AgNPs and reported AgNPs in 4-NP reduction using $NaBH_4$ at room temperature

Reductant-Stabilizer	[Ag] (mg/L)	[4-NP] (mM)	[$NaBH_4$]/[4-NP]	k (min^{-1})	Reference
Citrate-glycerol	0.10	0.14	175/1	0.4673 (± 0.0095)*	This study
Glycerol-PVP	0.10	0.14	175/1	0.1064	Nguyen et al. (2025)
Musa paradisiaca L. peel extract	43.2	0.10	200/1	0.2230	Phan et al. (2024)
Mono-thioureidophosphonate	15.7	0.12	200/1	0.1656	El-Tantawy et al. (2023)
Bis-thioureidophosphonate	17.0	0.12	200/1	0.1146	El-Tantawy et al. (2023)
Aloe vera leaf extract	3333	0.08	200/1	0.0906	Riaz et al. (2022)
Acacia nilotica stem extract	1666	0.08	200/1	0.0806	Shah et al. (2020)
Allium ampeloprasum L. leaf extract	0.53	0.13	2500/1	0.2595	Khoshnamvand et al. (2019)
Trachyspermum ammi (*Ajwain*) seeds extract	3.57	0.05	300/1	0.3454	Chouhan et al. (2017)
$NaBH_4$- Polyguanidino oxanorbornene (PG-5K)	4.0	0.12	100/1	0.33	Baruah et al. (2013)

Note: *A mean value (± standard deviation) from triplicate measurements (n = 3).

route exhibit a good catalytic efficacy by achieving the higher pseudo-first-order rate constant (k) while operating at a reduced metallic loading and a minimized [$NaBH_4$]/[4-NP] molar ratio. It is important to note that the literature comparison presented in Table 1 serves primarily to provide a general overview of AgNPs catalytic efficiency. A direct quantitative ranking remains inherently limited due to the disparate experimental conditions across the reported studies, such as variations in initial reactant concentrations, solution pH, stirring rates, and operating temperatures. Furthermore, because several referenced works omit specific parameters regarding active surface sites or early-stage initial reaction rates, standardized metrics like mass-normalized activity or turnover frequency (TOF) could not be uniformly calculated. Consequently, these values should be interpreted as qualitative indicators of performance rather than a direct benchmarking baseline.

Beyond initial kinetic efficiency, the operational longevity of the nano-colloid was verified across consecutive reusability trials (Figure 5). The catalyst maintained robust, stable conversion efficiency over three consecutive cycles, a durability directly ascribed to the structural

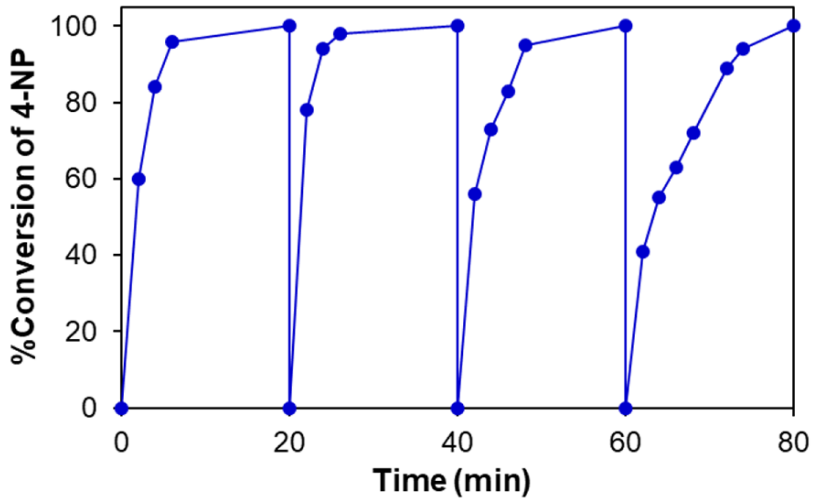

Figure 5. Stability evaluation of AgNPs catalyst over 4 consecutive cycles in 4-NP reduction using $NaBH_4$ at room temperature

immobilization of the metallic cores within the viscous, citrate-glycerol network which effectively suppresses particle agglomeration. However, a progressive decline in catalytic activity was observed during the fourth cycle, characterized by an extended reaction timeline for complete 4-NP decolorization. This attenuation in performance is indicative of progressive active-site passivation; specifically, the accumulation and strong chemisorption of metaborate byproducts onto the nanoparticle surfaces creates a physical mass-transfer barrier, blocks the exposed metallic facets, and consequently restricts reactant accessibility to the active catalytic centers.

CONCLUSIONS

This work optimized a sustainable citrate-glycerol framework to synthesize AgNPs with high uniformity and a sub-10 nm particle size (averaging 9.5 nm). These nanoparticles exhibited high efficiency in the catalytic reduction of 4-NP under mild ambient conditions. Being able to turn toxic 4-NP into a useful industrial chemical like 4-AP within six minutes, this work demonstrates the potential of citrate-glycerol-assisted synthesis for environmentally oriented catalytic applications. However, several factors require further investigation, such as the proposed mechanistic pathways warrant deeper validation, and the material's recyclability currently remains limited.

Although this method yields highly stable and uniform nanoparticles, practical challenges remain regarding its industrial scale-up. The low operating concentration of the colloid limits mass output unless substantial solvent volumes are processed. Besides, managing fluid dynamics and uniform thermal distribution within the viscous polyol matrix is critical to preventing localized over-nucleation and subsequent particle aggregation. Future scale-up strategies must therefore pivot toward continuous-flow chemistry.

Acknowledgements

This research is funded by Vietnam National University Ho Chi Minh City (VNU-HCM) under grant number: B2024-20-17. We acknowledge Ho Chi Minh City University of Technology (HCMUT), VNU-HCM for supporting this study.

REFERENCES

1. Ahmad, I., Khan, M.N., Hayat, K., Ahmad, T., Shams, D.F., Khan, W., Tirth, V., Rehman, G., Muhammad, W., Elhadi, M., Alotaibi, A., Shah, S.K. (2024). Investigating the antibacterial and anti-inflammatory potential of polyol-synthesized silver nanoparticles. *ACS Omega*, *9*(11), 13208–13216. https://doi.org/10.1021/acsomega.3c09851
2. Ayad, A.I., Luart, D., Dris, A.O., Guénin, E. (2020). Kinetic analysis of 4-nitrophenol reduction by "water-soluble" palladium nanoparticles. *Nanomaterials*, *10*(6), 1169. https://doi.org/10.3390/nano10061169
3. Baruah, B., Gabriel, G.J., Akbashev, M.J., Booher, M.E. (2013). Facile synthesis of silver nanoparticles stabilized by cationic polynorbornenes and their catalytic activity in 4-nitrophenol reduction. *Langmuir*, *29*(13), 4225–4234. https://doi.org/10.1021/la305068p
4. Boulkhessaim, S., Gacem, A., Khan, S.H., Amari, A., Yadav, V.K., Harharah, H.N., Elkhaleefa, A.M., Yadav, K.K., Rather, S.U., Ahn, H.J., Jeon, B.H. (2022). Emerging trends in the remediation of persistent organic pollutants using nanomaterials and related processes: A review. *Nanomaterials*, *12*(13), 2148. https://doi.org/10.3390/nano12132148
5. Bruna, T., Maldonado-Bravo, F., Jara, P., Caro, N. (2021). Silver nanoparticles and their antibacterial applications. *International Journal of Molecular Sciences*, *22*(13), 7202. https://doi.org/10.3390/ijms22137202
6. Chouhan, N., Ameta, R., Meena, R.K. (2017). Biogenic silver nanoparticles from Trachyspermum ammi (Ajwain) seeds extract for catalytic reduction of p-nitrophenol to p-aminophenol in excess of $NaBH_4$. *Journal of Molecular Liquids*, *230*, 74–84. https://doi.org/10.1016/j.molliq.2017.01.003
7. Dang-Bao, T., Favier, I., Gómez, M. (2021). Metal nanoparticles in polyols: bottom-up and top-down syntheses and catalytic applications. In: K. Philippot, A. Roucoux (Eds), Nanoparticles in Catalysis: Advances in Synthesis and Applications. Wiley-VCH. https://doi.org/10.1002/9783527821761.ch5
8. Dang-Bao, T., Le, N.H., Lam, H.H. (2022). Tuning polyol-mediated process towards augmentation of zero-valent copper nanoparticles. *Chemical Engineering Transactions*, *97*, 331-336. https://doi.org/10.3303/CET2297056
9. Dang-Bao, T., Nguyen, T.S., Tran-Dinh, N.T., Lam, H.H., Phan, H.P. (2023). Taking advance of isotropic-to-anisotropic morin-modified silver nanoparticles for simultaneous colorimetric sensing of trivalent chromium and iron ions. *Chemical Physics Impact*, *6*, 100245. https://doi.org/10.1016/j.chphi.2023.100245

10. Das, T.K., Das, N.C. (2022). Advances on catalytic reduction of 4-nitrophenol by nanostructured materials as benchmark reaction. *International Nano Letters*, *12*(3), 223–242. https://doi.org/10.1007/s40089-021-00362-w
11. Dong, H., Chen, Y.C., Feldmann, C. (2015). Polyol synthesis of nanoparticles: status and options regarding metals, oxides, chalcogenides, and non-metal elements. *Green Chemistry*, *17*(8), 4107–4132. https://doi.org/10.1039/C5GC00943J
12. El-Tantawy, A.I., Elsaeed, S.M., Neiber, R.R., Eisa, W.H., Aleem, A.A.H.A., El-Hamalawy, A.A., Maize, M.S. (2023). Silver nanoparticles-based thioureidophosphonate composites: Synthesis approach and their exploitation in 4-nitrophenol reduction. *Surfaces and Interfaces*, *40*, 103006. https://doi.org/10.1016/j.surfin.2023.103006
13. Fiévet, F., Ammar-Merah, S., Brayner, R., Chau, F., Giraud, M., Mammeri, F., Peron, J., Piquemal, J.Y., Sicard, L., Viau, G. (2018). The polyol process: a unique method for easy access to metal nanoparticles with tailored sizes, shapes and compositions. *Chemical Society Reviews*, *47*(14), 5187-5233. https://doi.org/10.1039/C7CS00777A
14. Helmlinger, J., Heise, M., Heggen, M., Ruck, M., Epple, M. (2015). A rapid, high-yield and large-scale synthesis of uniform spherical silver nanoparticles by a microwave-assisted polyol process. *RSC Advances*, *5*(112), 92144–92150. https://doi.org/10.1039/C5RA20446A
15. Jamkhande, P.G., Ghule, N.W., Bamer, A.H., Kalaskar, M.G. (2019). Metal nanoparticles synthesis: An overview on methods of preparation, advantages and disadvantages, and applications. *Journal of Drug Delivery Science and Technology*, *53*, 101174. https://doi.org/10.1016/j.jddst.2019.101174
16. Kästner, C., Thünemann, A.F. (2016). Catalytic reduction of 4-nitrophenol using silver nanoparticles with adjustable activity. *Langmuir*, *32*(29), 7383–7391. https://doi.org/10.1021/acs.langmuir.6b01477
17. Khoshnamvand, M., Huo, C., Liu, J. (2019). Silver nanoparticles synthesized using Allium ampeloprasum L. leaf extract: characterization and performance in catalytic reduction of 4-nitrophenol and antioxidant activity. *Journal of Molecular Structure*, *1175*, 90–96. https://doi.org/10.1016/j.molstruc.2018.07.089
18. Kumar, A., Savanur, M.R.S., Singh, S.K., Singh, J., Bhattacharya, S., Asnani, K., Kumar, B., Kumar, M., Kumar, S. (2025). Recent advances in silver nanoparticles-catalyzed reactions. *ChemistrySelect*, *10*(5), e202403655. https://doi.org/10.1002/slct.202403655
19. Le, V.L., Huynh, T.B., Lam, H.H., Nguyen, M.T.K., Dang-Bao, T. (2025). Glycerol-mediated synthesis of monodisperse sub-10 nm selenium nanoparticles: An eco-friendly and sustainable route. *Journal of Ecological Engineering*, *26*(11), 175–184. https://doi.org/10.12911/22998993/207910
20. Ly, M.T., Dang-Bao, T., Nguyen, M.T.K., Lam, H.H., Tran, T.K.A., Phan, H.P. (2024). Exploring a surface-capping role of carboxymethyl cellulose for the synthesis of silver nanoparticles via the induction period in a catalytic hydrogenation. *Journal of Molecular Structure*, *1309*, 138274. https://doi.org/10.1016/j.molstruc.2024.138274
21. Mejía, Y.R., Bogireddy, N.K.R. (2022). Reduction of 4-nitrophenol using green-fabricated metal nanoparticles. *RSC Advances*, *12*(29), 18661–18675. https://doi.org/10.1039/D2RA02663E
22. Mohaghegh, S., Osouli-Bostanabad, K., Nazemiyeh, H., Javadzadeh, Y., Parvizpur, A., Barzegar-Jalali, M., Adibkia, K. (2020). A comparative study of eco-friendly silver nanoparticles synthesis using Prunus domestica plum extract and sodium citrate as reducing agents. *Advanced Powder Technology*, *31*(3), 1169–1180. https://doi.org/10.1016/j.apt.2019.12.039
23. Moradi, F., Sedaghat, S., Moradi, O., Salmanabadi, S.A. (2021). Review on green nano-biosynthesis of silver nanoparticles and their biological activities: With an emphasis on medicinal plants. *Inorganic and Nano-Metal Chemistry*, *51*(1), 133–142. https://doi.org/10.1080/24701556.2020.1769662
24. Neal, R.D., Inoue, Y., Hughes, R.A., Neretina, S. (2019). Catalytic reduction of 4-nitrophenol by gold catalysts: the influence of borohydride concentration on the induction time. *The Journal of Physical Chemistry C*, *123*(20), 12894–12901. https://doi.org/10.1021/acs.jpcc.9b02396
25. Nguyen, V.H., Lam, H.H., Nguyen, M.T.K., Do, T.A.S., Phan, H.P., Dang-Bao, T. (2025). A clear-cut synthesis of silver nanoparticles using glycerol as a multipurpose medium toward catalytic hydrogenation and antibacterial. *JCIS Open*, *19*, 100141. https://doi.org/10.1016/j.jciso.2025.100141
26. Nguyen-Huynh, N.P, Phan, H.P., Lam, H.H., Do, T.A.S., Nguyen, P.T.D., Tran, T.K.A., Reina, A., Dang-Bao, T. (2025). Chromotropic acid-activated silver nanoparticles: a convenient colorimetric sensor for selective determination of divalent and trivalent iron ions. *Chemical Papers*, *79*, 6147–6158. https://doi.org/10.1007/s11696-025-04180-8
27. Oprica, L., Andries, M., Sacarescu, L., Popescu, L., Pricop, D., Creanga, D., Balasoiu, M. (2020). Citrate-silver nanoparticles and their impact on some environmental beneficial fungi. *Saudi Journal of Biological Sciences*, *27*(12), 3365–3375. https://doi.org/10.1016/j.sjbs.2020.09.004
28. Phan, H.P., Nguyen, T.T.N., Hua, T.K.C., Tu, Q.D., Nguyen, M.T.K., Lam, H.H., Tran, T.K.A., Dang-Bao, T. (2024). *Musa paradisiaca* L. peel

extract-bioinspired anisotropic nano-silver with the multipurpose of hydrogenation eco-catalyst and antimicrobial resistance. *Heliyon*, *10*(16), e36037. https://doi.org/10.1016/j.heliyon.2024.e36037

29. Polte, J. (2015). Fundamental growth principles of colloidal metal nanoparticles–a new perspective. *CrystEngComm*, *17*(36), 6809–6830. https://doi.org/10.1039/C5CE01014D
30. Riaz, M., Sharafat, U., Zahid, N., Ismail, M., Park, J., Ahmad, B., Rashid, N., Fahim, M., Imran, M., Tabassum, A. (2022). Synthesis of biogenic silver nanocatalyst and their antibacterial and organic pollutants reduction ability. *ACS Omega*, *7*(17), 14723–14734. https://doi.org/10.1021/acsomega.1c07365
31. Selvam, K., Prasath, A.R., Alanazi, A.K. (2026). A review of recent developments in green synthesis of silver nanoparticles: antioxidant and antibacterial applications. *Microscopy Research and Technique*, *89*(1), 134–147. https://doi.org/10.1002/jemt.70060
32. Shah, Z., Hassan, S., Shaheen, K., Khan, S.A., Gul, T., Anwar, Y., Al-shaeri, M.A., Khan, M., Khan, R., Haleem, M.A., Suo, H. (2020). Synthesis of AgNPs coated with secondary metabolites of Acacia nilotica: An efficient antimicrobial and detoxification agent for environmental toxic organic pollutants. *Materials Science and Engineering: C*, *111*, 110829. https://doi.org/10.1016/j.msec.2020.110829
33. Shahbazi, N., Zare-Dorabei, R. (2019). A facile colorimetric and spectrophotometric method for sensitive determination of metformin in human serum based on citrate-capped gold nanoparticles: central composite design optimization. *ACS Omega*, *4*(17), 17519–17526. https://doi.org/10.1021/acsomega.9b02389
34. Sharma, K., Kaushal, S., Jain, A., Sami, M.H., Kumar, S., Tariq, H., Bano, K., Aggarwal, S., Kumar, R., Singh, P.P. (2024). A comprehensive review on biogenic synthesis of bimetallic nanoparticles and their application as catalytic reduction of 4-nitrophenol. *Chemical Papers*, *78*(5), 2757–2782. https://doi.org/10.1007/s11696-024-03323-7
35. Tessema, B., Gonfa, G., Hailegiorgis, S.M., Prabhu, S.V., Manivannan, S. (2023). Synthesis and characterization of silver nanoparticles using reducing agents of bitter leaf (*Vernonia amygdalina*) extract and tri-sodium citrate. *Nano-Structures & Nano-Objects*, *35*, 100983. https://doi.org/10.1016/j.nanoso.2023.100983
36. Thach-Nguyen, R., Lam, H.H., Phan, H.P., Dang-Bao, T. (2022). Cellulose nanocrystals isolated from corn leaf: straightforward immobilization of silver nanoparticles as a reduction catalyst. *RSC Advances*, *12*(54), 35436–35444. https://doi.org/10.1039/d2ra06689k
37. Thanh, N.T., Maclean, N., Mahiddine, S. (2014). Mechanisms of nucleation and growth of nanoparticles in solution. *Chemical Reviews*, *114*(15), 7610–7630. https://doi.org/10.1021/cr400544s
38. Tran, Q.H., Phan, H.P., Lam, H.H., Nguyen, P.T.D., Do, T.A.S., Tran, T.K.A., Dang-Bao, T. (2025). Glycerol-made ultrasmall platinum nanoparticles dispersed on eggshell-derived hydroxyapatite as a stable and long-term reduction catalyst. *Results in Engineering*, *26*, 105523. https://doi.org/10.1016/j.rineng.2025.105523
39. Tran, T.H., Nguyen, P.T.D., Tran, T.K.A., Dang-Bao, T. (2025). Glycerol-promoted synthesis of stable copper nanoparticles and their size-dependent catalytic reduction of 4-nitrophenol. *Results in Chemistry*, *18*, 102772. https://doi.org/10.1016/j.rechem.2025.102772
40. Tripathi, N., Goshisht, M.K. (2022) Recent advances and mechanistic insights into antibacterial activity, antibiofilm activity, and cytotoxicity of silver nanoparticles. *ACS Applied Bio Materials*, *5*(4), 1391-1463. https://doi.org/10.1021/acsabm.2c00014
41. Wang, J., Yin, J., Peng, D., Zhang, X., Shi, Z., Li, W., Shi, Y., Sun, M., Jiang, N., Cheng, B., Meng, X., Liu, R. (2025). 4-Nitrophenol at environmentally relevant concentrations mediates reproductive toxicity in *Caenorhabditis elegans* via metabolic disorders-induced estrogen signaling pathway. *Journal of Environmental Sciences*, *147*, 244–258. https://doi.org/10.1016/j.jes.2023.09.032
42. Wolf, J.B., Stawski, T.M., Smales, G.J., Thünemann, A.F., Emmerling, F. (2022). Towards automation of the polyol process for the synthesis of silver nanoparticles. *Scientific Reports*, *12*(1), 5769. https://doi.org/10.1038/s41598-022-09774-w
43. Zhang, Z., Yu, Y., Xi, H., Zhou, Y. (2022). Inhibitory effect of individual and mixtures of nitrophenols on anaerobic toxicity assay of anaerobic systems: Metabolism and evaluation modeling. *Journal of Environmental Management*, *304*, 114237. https://doi.org/10.1016/j.jenvman.2021.114237
44. Zhao, T., Sun, R., Yu, S., Zhang, Z., Zhou, L., Huang, H., Du, R. (2010). Size-controlled preparation of silver nanoparticles by a modified polyol method. *Colloids and Surfaces A: Physicochemical and Engineering Aspects*, *366*(1–3), 197–202. https://doi.org/10.1016/j.colsurfa.2010.06.005